Turk Neurosurg, 2024

Original Investigation

DOI: 10.5137/1019-5149.JTN.44104-23.2

Received: 09.04.2023
Accepted: 08.12.2023

Published Online: 23.10.2024

Anatomy of the Petrosphenoidal Ligament and Its Relationship with the Abducens Nerve in Newborn Cadavers

Burak Oguzhan KARAPINAR[1], Aymen Ahmed WARILLE[2], Orhan BAS[3], Mehmet EMIRZEOGLU[2]

[1]Ondokuz Mayıs University, Vocational School of Health Services, Department of Medical Services and Techniques, Samsun, Türkiye
[2]Ondokuz Mayıs University, Faculty of Medicine, Department of Anatomy, Samsun, Türkiye
[3]Samsun University, Faculty of Medicine, Department of Anatomy, Samsun, Türkiye

Corresponding author: Burak Oguzhan KARAPINAR ✉ burakkarapinar@hotmail.com

ABSTRACT

AIM: To examine the anatomy of the petrosphenoidal ligament (PSL) and its relationship with the abducens nerve (AN) in newborn cadavers.

MATERIAL and METHODS: Using 10 formalin-fixed newborn cadavers, 20 PSLs and ANs on both sides were examined. The structure of each PSL, its morphometric features, and its relationship with the AN were evaluated. For the morphometric measurements, photographs were taken in macro mode and then the ImageJ program was used.

RESULTS: The PSL was usually shaped like a butterfly. The structures of all the ligaments were complete. The PSL was attached to the petrous apex posteriorly and to the clivus or posterior clinoid process (PCP) anteriorly. The mean PSL length was 6.58±1.4 mm. The mean width of the ligament's attachment to the petrous apex was 3.12±0.63 mm. The mean width of the ligament's attachment to the PCP or clivus was 3.12±0.5 mm. The AN was located below the PSL in all the samples. It was usually situated in the 1/3 lateral part under the PSL (70%). The mean diameter of the AN, as located under the ligament, was 0.8±0.12 mm.

CONCLUSION: The PSL serves as an important anatomical landmark in the petroclival region. In addition, AN is closely adjacent to many anatomical structures such as the trigeminal nerve and internal carotid artery. The increased knowledge obtained through this study on newborn cadavers concerning the anatomy of the PSL and its relationship with the AN will help increase the success of surgical procedures and reduce surgical complications.

KEYWORDS: Petrosphenoidal ligament, Abducens nerve, Petroclival ligament, Petroclival region

ABBREVIATIONS: AN: Abducens nerve, **PSL:** Petrosphenoidal ligament, **PCP:** Posterior clinoid process

INTRODUCTION

The petrosphenoidal ligament (PSL), located in the petroclival region, was initally described in 1859 by the Russian physician and anatomist Wenzel Gruber. PSL is also termed as petroclival ligament, Gruber's ligament, or posterior petroclinoid ligament (5,22,27). The PSL is a fibrous bundle that is situated the meningeal and periosteal layers of the dura mater (15). It usually extends anteriorly from the lateral border of the upper section of the clivus or the posterior clinoid process (PCP) to the petrous apex. It can be duplicated, Y-shaped or arranged in a butterfly or triangle pattern in a single band (Figure 1-3) (8,10,15,22). In 78% of the specimens examined by Icke et al., the narrow ends of the PSL were shaped like a butterfly (8).

The superolateral boundary of Dorello's canal is formed by the PSL (12,26). In 1859, Gruber described Dorello's canal as a pathway located between the endosteal and meningeal dural leaves of the petroclival region and that extends from the petroclival entry point of the dura to the posterior end of the cavernous sinus. (1,21). Moreover, Dorello's canal contains

Burak Oguzhan KARAPINAR : 0000-0001-9005-5504
Aymen Ahmed WARILLE : 0000-0002-1035-1264
Orhan BAS : 0000-0002-7449-2699
Mehmet EMIRZEOGLU : 0000-0002-5038-0473

the abducens nerve (AN), the dorsal meningeal branch of the meningohypophyseal trunk and the inferior petrosal sinus. (Figure 1; 2A, B; 3) (14,16,17). The AN divides into three parts when it travels from the brainstem to the orbit. The subarachnoid space houses the initial part of the AN, which runs from the medullopontine sulcus to the dura mater and extends laterally to the clivus. The second part of the AN is that which becomes intracavernous after puncturing of the dura mater and then runs along the lateral aspect of the internal carotid artery. Via Dorello's canal, which is underneath the PSL, the AN travels to the second part. The third part of the AN lies within the orbit. Through the superior orbital fissure, it enters the orbit and travels to the lateral rectus muscle (18,19,29). The basilar artery's transverse branch, the petrous apex's pointed upper edge, and the ossified PSL may compress the AN, which is extremely sensitive to such trauma. In addition, many clinical illnesses, such as intracranial hypertension, malignancies of the skull base, and vascular and inflammatory ailments, can impact the AN either directly or indirectly (6,13,18,26).

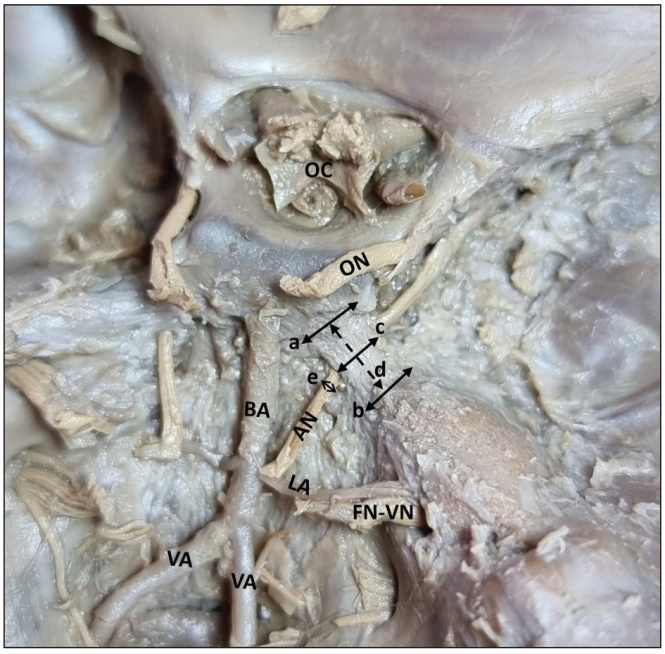

Figure 1: Morphometric measurements of PSL and AN. **A)** Width of the PSL at the clivus or PCP, **B)** Width of the PSL at the petrous apex, **C)** Width of the narrowest section of the PSL, **D)** Lenght of the PSL, **(e):** Diamater of the AN, **AN:** Abducens nerve, **BA:** Basilar artery, **FN:** Fascial nerve, **LA:** Labyrinthine artery, **OC:** optic chiasm, **ON:** Oculomotor nerve, **VA:** Vertebral artery, **VN:** Vestibulocochlear nerve.

The present study sought to assess the morphological and morphometric features of the PSL in newborn cadavers and to determine the relationship between the PSL and the AN. According to a review of the literature, this study is the first to examine the microanatomy of the PSL and its relationship with the AN in newborn cadavers. The increased knowledge of the microanatomy of the PSL and its relationship with surrounding structures, especially in newborn cadavers, generated in this study will help increase the success of surgery in the petroclival region and reduce surgical complications.

MATERIAL and METHODS

This study was carried out with the approval of the Ondokuz Mayıs University Clinical Research Ethics Committee (Decision no. 2022/390).

In this study, 10 newborn cadavers fixed with 10% formalin were used. A total of 20 PSLs and ANs from the 10 cadavers, on both the left and right sides, were examined. Clinical research ethics committee permission was obtained to conduct the study. To examine the PSL and AN structures, the following protocols were applied to each newborn cadaver.

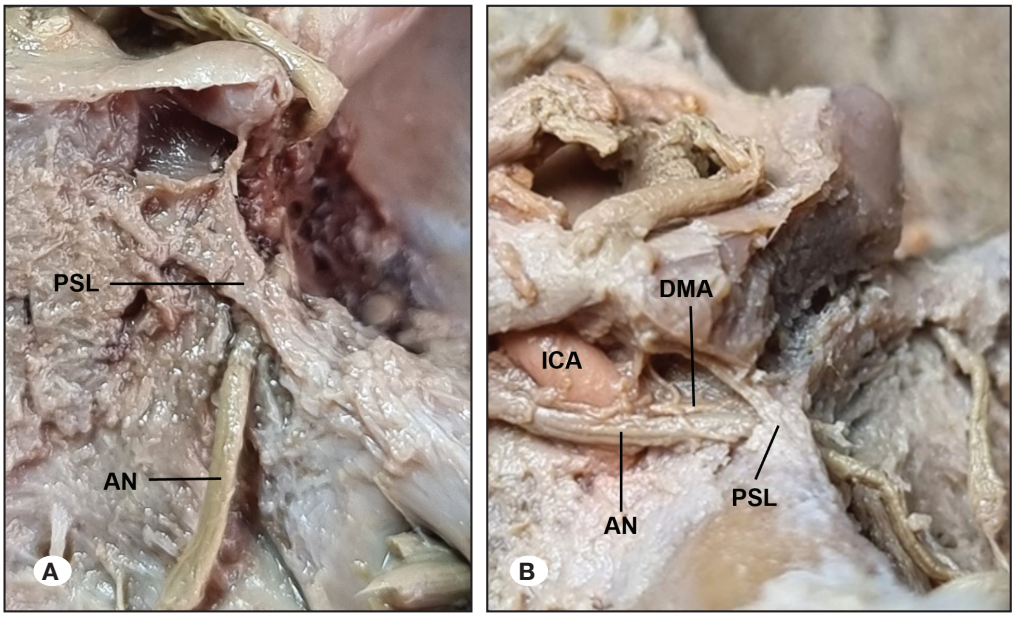

Figure 2: A) Butterfly shaped PSL, **B)** Y shaped PSL, The anterior attachment of the PSL is divided into two parts. One part attaches to the PCP and the other part to the clivus **PSL:** Petrosphenoidal ligament, **AN:** Abducens nerve, **ICA:** Internal carotid artery, **DMA:** Dorsal meningeal artery.

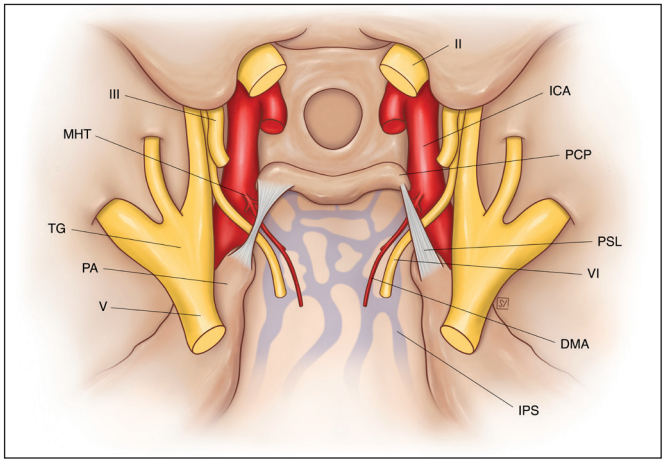

Figure 3: The left PSL represents the butterfly-shaped form and the right PSL represents the triangular-shaped form. **II:** Optic nerve, **III:** Oculomotor nerve, **V:** Trigeminal nerve, **VI:** Abducens nerve, **DMA:** Dorsal meningeal artery, **ICA:** Internal carotid artery, **IPS:** Inferior petrosal sinus, **MHT:** Meningohypophyseal trunk, **PA:** Petrous apex, **PCP:** Posterior clinoid process, **PSL:** Petrosphenoidal ligament, **TG:** Trigeminal ganglion.

To reach the base of the skull, a transverse skin incision was first made around the head, starting 1 cm above the supraorbital edge and then extending from the upper glabella anteriorly to the inion posteriorly. The calvaria was made visible by removing the skin. Next, following cranial osteotomy using bone scissors, the calvaria was removed and the dura mater made visible. After the dura mater was reflected, the cerebral hemispheres were carefully removed so that the optic chiasm and cranial nerves were preserved at the base of the skull. The tentorium cerebelli was then dissected, starting near both the transverse sinuses. Subsequently, the cerebellum, mesencephalon, pons, and medulla oblongata were removed. In the internal cranial base, both the vessels and nerves were preserved and the region was roughly dissected. Finally, the AN was dissected in and below the dura mater up to the superior orbital fissure via microdissection performed using a LEICA CLS 100 stereo microscope in the anatomy dissection laboratory. Moreover, the PSL was also dissected in this region and made visible for the morphological and morphometric evaluations.

The structure of the PSL, the locations of its origin and insertion, its width of the points of origin and insertion, the location and width of its narrowest part, and its total length were evaluated. The diameter and location of the AN under the PSL, as well as whether it was attached to or separate from the ligament, were also examined. For the morphometric measurements, photographs were taken in macro mode and then the ImageJ program was used. The right–left differences in the morphometric features of the AN and PSL were examined. Additionally, the mean and standard deviation of each morphometric measurement were calculated. Student's t-test was used to perform the statistical analyses. $p<0.05$ was considered statistically significant.

RESULTS

Morphological Findings

The anterior end of the PSL is attached to the PCP and upper portion of the clivus, while its posterior end is attached to the petrous apex. The posterior attachment point of the PSL was found to be the petrous apex in all the samples. Moreover, the anterior attachment point of the PSL was determined to be in the clivus in 70% of the samples and in the PCP in 20%. In the remaining 10%, the PSL was Y-shaped and attached to both the PCP and the clivus. These findings lead us to conclude that the PSL is generally triangular or butterfly-shaped. Indeed, in 75% of the samples, it was butterfly-shaped. In these butterfly-shaped ligaments, the narrowest part of the ligament was located in the middle, while the widest part was located at the point of attachment to the PCP and petrous apex. In 15% of the samples, the PSL was triangular. In these ligaments, the narrowest part was located at the point of attachment to the clivus or petrous apex. Furthermore, the PSL had a bilateral butterfly shape in 70% of the samples, a bilateral Y shape in 10%, and a bilateral triangular shape in 10%. One side of the remaining 10% had a triangular shape, while the other had a butterfly shape (Figure 1-3). Our conclusions regarding the overall shape of the PSL are summarized in Table I.

When the location of the AN under the PSL was examined, it was observed that the AN was located in the lateral 1/3 in 75% of the samples, in the middle 1/3 in 15%, and in the medial 1/3 in 10%. The AN was asymmetrical in 30% of the samples, while it was symmetrical and located in the lateral 1/3 in 70%. In addition, the AN was attached to the PSL in 45% of the samples and separate from the PSL in 55%.

Morphometric Measurements

The mean overall length of the PSL was found to be 6.58±1.4 mm, while the mean lengths of the right and left PSLs were 6.63 ± 1.58 mm and 6.52 ± 1.29 mm, respectively. The PCP attachment band was used to measure the lengths of the Y-shaped PSLs.

The mean overall width of the PSL at the anterior point of attachment to the PCP or clivus was 3.12 ± 0.5 mm. The mean widths of the right and left PSLs at the anterior point of attachment to the PCP or clivus were 3.2 ± 0.36 mm and 2.98 ± 0.62 mm, respectively. The mean overall width of the PSL at the posterior point of attachment to the petrous apex was 3.12 ± 0.63 mm. The mean widths of the right and left PSLs at the posterior point of attachment to the petrous apex were 3.03 ± 0.68 mm and 3.21 ± 0.6 mm, respectively. The mean overall length of the narrowest part of the PSL was 2.03 ± 0.55 mm. The mean lengths of the narrowest part of the right and left PSLs were 1.95 ± 0.63 mm and 2.1 ± 0.48 mm, respectively (Table I).

The mean diameter of the AN below the PSL was 0.8 ± 0.12 mm. The mean diameters of the right and left ANs under the PSL were 0.81 ± 0.13 mm and 0.8 ± 0.12 mm, respectively. There was no statistically significant difference observed between the morphometric features of the right and left PSLs ($p>0.05$).

Table I: Length of PSL, Width of the PSL at the Clivus-PCP and Petrous Apex, Widht of the Narrowest Section of the PSL, Diamater of the AN Below the PSL

	Right	Left	Total
Length of the PSL (mm)			
Mean ± SD (Range of length)	6.63 ± 1.58 (3.61-8.54)	6.52 ± 1.29 (3.73-7.68)	6.58 ± 1.4 (3.61-8.54)
PSL's width at the clivus or PCP (mm)			
Mean ± SD (Range of width)	3.2 ± 0.36 (2.72-3.89)	2.98 ± 0.62 (2.3-4.02)	3.12 ± 0.5 (2.3-4.02)
PSL's width at the petrous apex (mm)			
Mean ± SD (Range of width)	3.03 ± 0.68 (1.37-3.79)	3.21 ± 0.6 (2.53-4.18)	3.12 ± 0.63 (1.37-4.18)
Width of the narrowest section of the PSL (mm)			
Mean ± SD (Range of width)	1.95 ± 0.63 (1.3-3.02)	2.1 ± 0.48 (1.56-2.89)	2.03 ± 0.55 (1.3-3.02)
Diamater of the AN (mm)			
Mean ± SD (Range of diamater)	0.81 ± 0.13 (0.65-1.05)	0.8 ± 0.12 (0.59-0.99)	0.8 ± 0.12 (0.59-1.05)

PSL: *Petrosphenidal ligament,* ***PCP:*** *Posterior clinoid process,* ***AN:*** *Abducens nerve,* ***SD:*** *Standard deviation* ***mm:*** *Milimete.*

DISCUSSION

The petroclival region, which is located at the intersection of the sphenoid, temporal, and occipital bones, is a highly complicated region of clinical significance. Thus, a thorough understanding of its microanatomy is necessary to ensure the success of surgery in the petroclival region and cavernous sinus. In the petroclival region, the PSL is recognized as a crucial structure, not only from an anatomical perspective but also in terms of surgical and endovascular practice. Dorello's canal and the PSL represent important surgical landmarks that help prevent injury to the AN during the removal of the meningiomas, chordomas, and pituitary adenomas from the petroclival region using transnasal surgical approaches (11,20,23). This study sought to determine the microanatomy of the PSL and its relationship with the AN in newborn cadavers. The morphometric findings revealed the PSLs in newborn cadavers to differ from those in adults, with the most common form of PSL in newborn cadavers being butterfly-shaped and the AN usually being located 1/3 laterally under the PSL.

Previous studies have examine the microanatomy of the PSLs in adult cadavers (6-8,10,11,15,22), while Kayaci et al. assessed the microanatomy of the PSLs in both adult and pediatric groups in their cadaver study (13). However, a review of the literature revealed the present study to be the first to investigate the morphometry and microanatomy of the PSLs in newborn cadavers.

Studies in the literature have shown that the morphological features of the PSL may differ. In these studies, Iaconetta et al., Özveren et al., and Liu et al. reported that this ligament is only butterfly-shaped (7,15,20). Icke et al., Destrieux et al., Kayacı et al., Iwanaga et al., Gutierrez et al., and Plutecki et al. found that the most common form of the PSL is butterfly-shaped, but it can also be triangular, Y-shaped, and duplicated (4,6,8,10,13,22). In our study, the most common form of the PSL was butterfly-shaped (75%), although we also encountered a triangular PSL (15%) and a Y-shaped PSL (10%).

As for the morphometric characteristics of the PSL, in a study on 10 adult cadavers, Joo et al. reported that the mean length of the PSL was 11.05 mm, the mean width of the PSL at the petrous apex was 3.0 mm, and the mean width of the PSL at the point of attachment to the PCP was 3.85 mm. They also found that the width of the narrowest part of the PSL was 2.05 mm (11). Iwanaga et al. studied 18 adult cadavers and determined the mean length of the PSL to be 9.50 ± 3.10 mm and the mean width of the narrowest part of the PSL to be 1.49 ± 0.61 mm (10). After examining 20 adult cadavers, Icke et al. reported the mean length of the PSL to be 13.4 ± 3.3 mm and the mean width of the PSL to be 4.2 ± 1.6 mm at the petrous apex and 6.1 ± 3.2 mm at the PCP. They further reported the mean width of the narrowest part of the PSL to be 2.0 ± 0.9 mm in the butterfly-shaped PSLs and 2.8 ± 2.3 mm in the triangular-shaped PSLs (8). In a study on eight adult cadavers, Özveren et al. found that the mean length of the PSL was 10.3 mm, while the mean width of the PSL was 3.8 mm at the petrous apex and 6.4 mm at the PCP, and they also found that the mean width of the narrowest part of the PSL was 2.7 mm (20). In their study on 50 adult cadavers, Iaconetta et al. observed the mean PSL length to be 13.31 ± 2.34 mm and the mean PSL width to be 5.48 ± 2.2 mm in the petrous apex and 4.27 ± 2.5 mm in the PCP. Moreover, the mean width at the narrowest part of the PSL was found to be 2.05 ± 1.8 mm (7). In their analysis of 17 adult cadavers and 12 pediatric cadavers, Kayacı et al. determined that the mean PSL length in the pediatric group was 7.0 ± 1.47 mm, while in the adult group it was 11.05 ± 2.95 mm (13). In the present study, the mean length of the PSL was 6.58 ± 1.4 mm and the mean width of the PSL was 3.12 ± 0.63 mm at the petrous apex and 3.12 ± 0.5 mm at the clivus or PCP. Additionally, the mean width of the narrowest part of the PSL was 2.03 ± 0.55

mm. It is important to note here that the anatomical features of the PSL change with the development of the clivus. Indeed, Kayacı et al. reported that the microanatomy of the PSL shows a significant difference when comparing children and adults ($p<0.001$) (13). The identified differences between our results and those of other studies are due to the fact that they were studied in different age groups.

In terms of case reports concerning the PSL, Karapinar et al. showed that the right and left PSLs can join at the clivus. They also emphasized that the possible variations should be determined prior to surgery being performed in the petroclival region (12). Furthermore, Zytkowski et al. found that some fibers of the anterior attachment of the PSL attach to the internal carotid artery. They suggested that this situation causes an atypical fixation for both the PSL and the internal carotid artery, meaning it is important to know such a variation in surgeries that require mobilization of the internal carotid artery (30).

Relationship between the PSL and the AN

The path of the AN in the petroclival area is specifically defined by the PSL. Dorello's canal is the area bordered by the PSL, the petrous apex, and the superolateral portion of the clivus to which the PSL is attached. According to prior reports, the clival arteries, inferior petrosal sinus, and AN all run via Dorello's canal (7,22). Our review of the literature did not identify any study that has examined the relationship between the PSL and the AN in newborn cadavers, although some studies have investigated this relationship in pediatric and adult cadavers (8,10,11,13,18,26).

The location of the AN beneath the PSL varies. The AN usually passes under the PSL and enters the cavernous sinus, although it can also enter the cavernous sinus by passing through or over the PSL (19). According to the findings of Umansky et al., the AN was located in the middle third (52%), lateral third (39%), or medial third (9%) of Dorello's canal (26). In the study by Özer et al., in 82.5% of cases, the AN was located in the lateral part of the 1/3 below the PSL, while in 12.5% of cases, it was located in the middle 1/3 below the PSL (18). Iwanaga et al. found that the AN crossed under the lateral 1/3 of the PSL in 19 cases (61.3%) and under the middle 1/3 in 12 cases (38.7%) (10). Joo et al. reported that in 95% of the 20 cadavers they examined, the AN crossed under the lateral 1/3 of the PSL (11). In these studies, the AN was mostly located in the lateral 1/3 part of the PSL. By contrast, Kayacı et al. showed that the AN mostly (67%) passed through the 1/3 medial part of the PSL in their pediatric cadaver group. They stated that this finding was related to the growth pattern of the clivus and to the AN being localized in the medial part of the PSL during the first 1.5 years of life, but as the age progressed, the clivus enlarges and the AN moves laterally (13). In the present study, despite examining newborn cadavers, we found that the AN was located in the lateral 1/3 of the PSL in 75% of cases. While this finding is similar to the findings of studies conducted on adult cadavers, it does not accord with the findings of Kayacı et al.'s study on pediatric cadavers (13).

With regard to the morphometric characteristics of the AN, Ozveren et al. reported the mean diameter of the AN under the PSL to be 1.5 mm, while Iwanaga et al. reported it to be 1.56 ± 0.35 mm (10,19). Ozer et al. found that the mean AN diameter was 1.3 ± 0.2 mm under the PSL (18). We determined the mean diameter of the AN under the PSL to be 0.8 ± 0.12 mm. Ozveren et al. reported that an accessory AN can be seen under the PSL and that it is not a very rare variation. If the variations of the AN are well known, the possibility of nerve injury during skull base surgeries and transvenous endovascular interventions will be reduced (19). Previous studies have also revealed that the accessory AN can pass over the PSL (7,11,19,29), which shows that the notion of the AN always passing through Dorello's canal is untrue. For this reason, Destrieux et al. named the region through which the AN passes "petroclival venous confluence" instead of the Dorello canal (4). Cases in which the AN branch passes over the PSL are more prone to injury during the transpetrosal surgical approach (19).

Duplication of the AN can also be observed in the petroclival region (7,11,18,19). This duplication may involve a subarachnoid nerve segment, and two different entry points of the nerve can sometimes be discerned. In addition, this duplication may be distal to the dura entry point of the nerve, meaning that a single nerve trunk enters the clival dura and then duplicates. Therefore, the possibility of an accessory abducens trunk should always be considered during surgical exploration of the petroclival region (28). The most non-mobile segment of the AN is located under the PSL and in Dorello's canal before it enters the cavernous sinus. Moreover, AN injuries are most common in this region, which can be explained by the fixation of the dural sheath of the nerve to the periosteal layer of the dura mater (2,28). For the surgical mobilization of the AN, anatomical fixation points should be considered.

The PSL can ossify, causing changes to the structure of the skull base. A bony bridge is formed by the PSL, which is ossified to varying degrees, from entirely to only partially. Ossification of the PSL usually occurs unilaterally (21,25,27). Touska et al. reported that PSL ossification increased with age and PSL ossification was not observed under 20 years of age (24). However, Clarke et al. identified an ossified PSL in a fetal skull and so determined that PSL ossification can occur at any age (3). In our study on newborn cadavers, no complete or partial ossification was found in any PSL. Ossification of the PSL may cause it to press on the AN, leading to the nerve being damaged. According to Tubbs et al., when treating patients who have unexplained occurrences of AN palsy, doctors should take the possibility of PSL ossification into consideration (25). Still, ossification of the PSL is not always harmful for the AN. In fact, Inal et al. demonstrated in a radiological study that an ossified PSL would play a protective role in relation to the AN and reduce the pressure on it in patients with increased head pressure syndrome (9).

CONCLUSION

The PSL serves as an important anatomical landmark in the petroclival region. It is also located closely adjacent to many anatomical structures, such as the AN, trigeminal nerve, and internal carotid artery. We believe that increasing

understanding of the microanatomy of the PSL and its relationship with neighboring anatomical structures such as the AN will significantly contribute to the success of surgical procedures in the petroclival region and reduce surgical complications.

ACKNOWLEDGEMENTS

In order for anatomical study to be done, the authors warmly thank those who contributed their bodies to science. The outcomes of such research could potentially advance human knowledge, which would then improve patient care. Our deepest gratitude is due to these contributors and their families.

We also acknowledge the support of the Turkish Council for Scientific and Technological Research under the 2211-A General Doctoral Scholarship.

We would like to thank Serap Yilmaz for her schematic drawing.

Declarations

Funding: The authors did not receive support from any organization for the submitted work.

Availability of data and materials: The data used to support the findings of this study are available from the corresponding author upon reasonable request.

Disclosure: The authors declare that there are no conflicts of interest relevant to this study.

AUTHORSHIP CONTRIBUTION

Study conception and design: BOK, OB
Data collection: BOK, OB
Analysis and interpretation of results: AAW, OB
Draft manuscript preparation: BOK, AAW
Critical revision of the article: ME, OB
Other (study supervision, fundings, materials, etc...): ME
All authors (BOK, AAW, OB, ME) reviewed the results and approved the final version of the manuscript.

REFERENCES

1. Ambekar S, Sonig A, Nanda A: Dorello's canal and gruber's ligament: Historical perspective. J Neurol Surg B Skull Base 73:430-433, 2012. https://doi.org/10.1055/s-0032-1329628
2. Barges-Coll J, Fernandez-Miranda JC, Prevedello DM, Gardner P, Morera V, Madhok R, Carrau RL, Snyderman CH, Rhoton AL Jr, Kassam AB: Avoiding injury to the abducens nerve during expanded endonasal endoscopic surgery: Anatomic and clinical case studies. Neurosurgery 67:144-154; discussion 154, 2010. https://doi.org/10.1227/01.NEU.0000370892.11284.EA
3. Clarke E, Golberg M, Smędra A, Mazur M, Mazurek A, Balawender K, Barszcz K, Żytkowski A: Bilateral caroticoclinoid foramen and unilateral abducens nerve canal found on the fetal skull-Case report. Transl Res Anat 29:100224, 2022. https://doi.org/10.1016/j.tria.2022.100224
4. Destrieux C, Velut S, Kakou MK, Lefrancq T, Arbeille B, Santini JJ: A new concept in Dorello's canal microanatomy: The petroclival venous confluence. J Neurosurg 87:67-72, 1997. https://doi.org/10.3171/jns.1997.87.1.0067
5. Gruber W: Beiträge zur Anatomie des Keilbeines und Schläfenbeines, 1859
6. Gutierrez S, Khan PA, Iwanaga J, Dumont AS, Tubbs RS: Review of the petroclinoid ligament. Kurume Med J 67:5-10, 2022. https://doi.org/10.2739/kurumemedj.MS671007
7. Iaconetta G, Fusco M, Cavallo LM, Cappabianca P, Samii M, Tschabitscher M: The abducens nerve: Microanatomic and endoscopic study. Neurosurgery 61:7-14; discussion 14, 2007. https://doi.org/10.1227/01.neu.0000289706.42061.19
8. Icke C, Ozer E, Arda N: Microanatomical characteristics of the petrosphenoidal ligament of Gruber. Turk Neurosurg 20:323-327, 2010. https://doi.org/10.5137/1019-5149.JTN.2921-10.0
9. Inal M, Muluk NB, Burulday V, Akgul MH, Ozveren MF, Celebi UO, Simsek G, Daphan B: Investigation of the calcification at the petroclival region through Multi-slice Computed Tomography of the skull base. J Craniomaxillofac Surg 44:347-352, 2016. https://doi.org/10.1016/j.jcms.2016.01.018
10. Iwanaga J, Altafulla JJ, Gutierrez S, Dupont G, Watanabe K, Litvack Z, Tubbs RS: The Petroclinoid Ligament: Its morphometrics, relationships, variations, and suggestion for new terminology. J Neurol Surg B Skull Base 81:603-609, 2020. https://doi.org/10.1055/s-0039-1692699
11. Joo W, Yoshioka F, Funaki T, Rhoton AL Jr: Microsurgical anatomy of the abducens nerve. Clin Anat 25:1030-1042, 2012. https://doi.org/10.1002/ca.22047
12. Karapinar BO, Warille AA, Bas O, Emirzeoglu M, Bilgic S: An atypical anatomical variation of the petrosphenoidal ligament in a newborn cadaver. Surg Radiol Anat 45:137-141, 2023. https://doi.org/10.1007/s00276-022-03072-w
13. Kayacı S, Ozveren MF, Bas O, Ayberk G, Aslan MN, Sam B, Arslan YK: Effect of clival bone growth on the localization of the abducens nerve at the petroclival region: A postmortem anatomical study. Surg Radiol Anat 43:953-959, 2021. https://doi.org/10.1007/s00276-021-02691-z
14. Li D, Tang J, Ren C, Wu Z, Zhang LW, Zhang JT: Surgical management of medium and large petroclival meningiomas: A single institution's experience of 199 cases with long-term follow-up. Acta Neurochir (Wien) 158:409-425; discussion 425, 2016. https://doi.org/10.1007/s00701-015-2671-6
15. Liu XD, Xu QW, Che XM, Mao RL: Anatomy of the petrosphenoidal and petrolingual ligaments at the petrous apex. Clin Anat 22:302-306, 2009. https://doi.org/10.1002/ca.20771
16. Maślanka K, Zielinska N, Tubbs RS, Haładaj R, Konschake M, Niemiec M, Olewnik Ł: The effect of morphological variability of Dorello's canal on surgical procedures - a review. Ann Anat 243:151939, 2022. https://doi.org/10.1016/j.aanat.2022.151939
17. Mortazavi MM, Griessenauer CJ, Krishnamurthy S, Verma K, Loukas M, Tubbs RS: The inferior petrosal sinus: A comprehensive review with emphasis on clinical implications. Childs Nerv Syst 30:831-834, 2014. https://doi.org/10.1007/s00381-014-2378-7

18. Ozer E, Icke C, Arda N: Microanatomical study of the intracranial abducens nerve: Clinical interest and surgical perspective. Turk Neurosurg 20:449-456, 2010. https://doi.org/10.5137/1019-5149.JTN.3303-10.1
19. Ozveren MF, Sam B, Akdemir I, Alkan A, Tekdemir I, Deda H: Duplication of the abducens nerve at the petroclival region: An anatomic study. Neurosurgery 52:645-652, 2003. https://doi.org/10.1227/01.NEU.0000048186.18741.3C
20. Ozveren MF, Uchida K, Aiso S, Kawase T: Meningovenous structures of the petroclival region: Clinical importance for surgery and intravascular surgery. Neurosurgery 50:829-836; discussion 836-827, 2002. https://doi.org/10.1097/00006123-200204000-00027
21. Özgür A, Esen K: Ossification of the petrosphenoidal ligament: multidetector computed tomography findings of an unusual variation with a potential role in abducens nerve palsy. Jpn J Radiol 33:260-265, 2015. https://doi.org/10.1007/s11604-015-0410-9
22. Plutecki D, Ostrowski P, Bonczar M, Iwanaga J, Walocha J, Pękala A, Szczepanek E, Tubbs RS, Loukas M, Wysiadecki G, Koziej M: The petroclinoid ligament: A meta-analysis of its morphometry and prevalence of mineralization with a review of the literature. Folia Morphol (Warsz) 82:487-497, 2023. https://doi.org/10.5603/FM.a2022.0082
23. Tomio R, Toda M, Sutiono AB, Horiguchi T, Aiso S, Yoshida K: Grüber's ligament as a useful landmark for the abducens nerve in the transnasal approach. J Neurosurg 122:499-503, 2015. https://doi.org/10.3171/2014.10.JNS132437
24. Touska P, Hasso S, Oztek A, Chinaka F, Connor SEJ: Skull base ligamentous mineralisation: Evaluation using computed tomography and a review of the clinical relevance. Insights Imaging 10:55, 2019. https://doi.org/10.1186/s13244-019-0740-8
25. Tubbs RS, Sharma A, Loukas M, Cohen-Gadol AA: Ossification of the petrosphenoidal ligament: Unusual variation with the potential for abducens nerve entrapment in Dorello's canal at the skull base. Surg Radiol Anat 36:303-305, 2014. https://doi.org/10.1007/s00276-013-1171-8
26. Umansky F, Elidan J, Valarezo A: Dorello's canal: A microanatomical study. J Neurosurg 75:294-298, 1991. https://doi.org/10.3171/jns.1991.75.2.0294
27. Wysiadecki G, Haładaj R, Polguj M, Żytkowski A, Topol M: Bilateral extensive ossification of the posterior petroclinoid ligament: An anatomical case report and literature review. J Neurol Surg A Cent Eur Neurosurg 80:122-126, 2019. https://doi.org/10.1055/s-0038-1666782
28. Wysiadecki G, Radek M, Tubbs RS, Iwanaga J, Walocha J, Brzeziński P, Polguj M: Microsurgical anatomy of the inferomedial paraclival triangle: Contents, topographical relationships and anatomical variations. Brain Sci 11:596, 2021. https://doi.org/10.3390/brainsci11050596
29. Zhang Y, Yu H, Shen BY, Zhong CJ, Liu EZ, Lin YZ, Jing GH: Microsurgical anatomy of the abducens nerve. Surg Radiol Anat 34:3-14, 2012. https://doi.org/10.1007/s00276-011-0850-6
30. Żytkowski A, Clarke E, Musiał A, Dubrowski A, Mazur M, Iwanaga J, Tubbs RS, Wysiadecki G: Atypical attachment of the petrosphenoidal (petroclival) ligament to the posterior genu of the cavernous internal carotid artery-Case report. Transl Res Anat 27:100185, 2022. https://doi.org/10.1016/j.tria.2022.100185